DISCRIMINATION OF INFECTED SILKWORM CHRYSALISES USING NEAR INFRARED SPECTROSCOPY COMBINED WITH MULTIVARIATE ANALYSIS DURING THE CULTIVATION OF *Cordyceps militaris*[**]

Y. Zhang [1,2], X. Wang [1], Ch. Wang [1], Y. Zhou [1], D. Pan [1], B. Luo [1*]

[1] National Research Center of Intelligent Equipment for Agriculture, Beijing, 100097, China; e-mail: luob@nercita.org.cn
[2] College of Equipment Agricultural Engineering at Henan University of Science and Technology, Luoyang, 471003, China

The objective of this study was to confirm whether near infrared spectroscopy could be used to discriminate the infected silkworm chrysalises. A total of 105 silkworm chrysalises – 65 infected and 40 uninfected – were collected at Beijing Shoucheng Agricultural Development Co., Ltd. Near infrared spectra were acquired at the head, chest, abdomen, and posterior belly of each silkworm chrysalis (both uninfected and infected). Three spectral pre-processing methods and four discrimination models were used to identify the uninfected and infected silkworm chrysalises. Results indicated that the PLS-DA model based on the spectra processed by multiplicative scatter correction (MSC) had the best discrimination performance (the prediction accuracy of calibration set and prediction set were 100 and 97.5%, respectively), and the head portion was the best position for the discrimination of uninfected and infected silkworm chrysalises. The overall conclusion was that the uninfected and infected silkworm chrysalises could be successfully identified by using near infrared spectroscopy technology in the cultivation of Cordyceps militaris.

Keywords: *Cordyceps militaris, multiplicative scatter correction, partial least square discriminant analysis.*

РАСПОЗНАВАНИЕ ЗАРАЖЕННЫХ ХРИЗАЛИДОВ ТУТОВОГО ШЕЛКОПРЯДА С ИСПОЛЬЗОВАНИЕМ СПЕКТРОСКОПИИ БЛИЖНЕГО ИК-ДИАПАЗОНА В СОЧЕТАНИИ С МНОГОМЕРНЫМ АНАЛИЗОМ ВО ВРЕМЯ КУЛЬТИВИРОВАНИЯ *Cordyceps militaris*

Y. Zhang [1,2], X. Wang [1], Ch. Wang [1], Y. Zhou [1], D. Pan [1], B. Luo [1*]

УДК 543.42:638.222.2

[1] Национальный исследовательский центр интеллектуальной техники для сельского хозяйства, Пекин, 100097, Китай; e-mail: luob@nercita.org.cn
[2] Колледж оборудования сельскохозяйственной инженерии Хэнаньского университета науки и технологий, Лоян, 471003, Китай

(Поступила 31 мая 2019)

Ближняя ИК-спектроскопия использована для распознавания зараженных хризалидов тутового шелкопряда. Всего 105 хризалидов тутового шелкопряда (65 инфицированных и 40 незараженных) собрано в пекинской компании Shoucheng Agricultural Development Co., Ltd. Спектры в ближнем ИК-диапазоне получены из областей головы, груди, живота и задней части брюшка каждого хризалида тутового шелкопряда (как незараженных, так и инфицированных). Для идентификации незараженных и инфицированных хризалидов тутового шелкопряда использованы три метода предварительной обработки спектров и четыре модели распознавания. Результаты показывают, что модель, использующая дискриминантный анализ на основе частичных наименьших квадратов и спектры, обработанные методом мультипликативной коррекции рассеяния, имеет лучшие характери-

[**] Full text is published in JAS V. 88, No. 1 (http://springer.com/journal/10812) and in electronic version of ZhPS V. 88, No. 1 (http://www.elibrary.ru/title_about.asp?id=7318; sales@elibrary.ru).

стики распознавания (точность прогнозирования калибровочного набора и набора прогнозирования 100 и 97.5%). Область головы оказалась наилучшим участком для распознавания незараженных и инфицированных хризалидов тутового шелкопряда. Неинфицированные и зараженные хризалиды шелкопряда могут быть успешно идентифицированы с помощью методов ближней ИК-спектроскопии при культивировании Cordyceps militaris.

Ключевые слова: *Cordyceps militaris, мультипликативная коррекция рассеяния, дискриминантный анализ на основе частичных наименьших квадратов.*

Introduction. *Cordyceps militaris*, also known as *Cordyceps*, chrysalis grass, and *Cordyceps polyarthra* Moller, belongs to the genus *Cordyceps*, family Cordycipitaceae, order Hypocreales, and phylum Ascomycota [1]. The organism is a species of *Cordyceps* fungi. Hosts of *C. militaris* include Bombycidae, Notodontidae, and Saturniidae family members of the order Lepidoptera. *C. militaris* has a complex structure, which is composed of sporocarp and sclerotium (body parts of worm or pupa). *C. militaris* and *C. sinensis* have been studied for decades to determine their pharmacological effect, components, and bioactivity. These organisms are an important part of health food and have been appreciated in China and worldwide over the past decades. Several studies have shown that *C. militaris* possesses a number of pharmacological activities (e.g. immunoregulation [2], antitumor [3], antivirus [4], and anti-infection actions [5]) and is widely used in the treatment of tumors, immunodeficiency, and even AIDS [6]. With the reduction of wild *C. sinensis*, *C. militaris* is an ideal substitute for *C. sinensis* because of their similar active components and pharmacological effects [7, 8]. Application research on scale production of *C. militaris* has attracted substantial attention worldwide [9].

Scale production of *C. militaris* generally includes selection of mycelium, preparation of culture medium, cultivation of the mycelium, optimization and disinfection of silkworm chrysalis, and inoculation and cultivation of *C. militaris*. The cultivation of *C. militaris* is an important part of industrial production. After inoculation, the silkworm chrysalis infected by *C. militaris* mycelium becomes rigid and is called the normal silkworm chrysalis (or uninfected silkworm chrysalis), which is infected by *C. militaris* mycelium and is not infected by other microbes, whereas the silkworm chrysalis infected by other microbes becomes softer and eventually festers and is known as the infected silkworm chrysalis. The difference between the two silkworm chrysalises usually appears 7–10 days after inoculation [10]. Given the infection caused by other microbes, which often cause mass contamination of *C. militaris,* finding infected silkworm chrysalis in a timely manner during the cultivation of *C. militaris* is difficult and thus leads to significant economic loss to *Cordyceps* production enterprises. Timely identification and recognition of infected silkworm chrysalis and adoption of appropriate measures can prevent cross-contamination of uninfected *C. militaris*. These methods are important for scale production of *C. militaris.*

Near infrared spectrum technology can fully use spectroscopic data under the whole spectral range or multi-wavelength for qualitative or quantitative analysis. Near infrared spectra technology is widely applied in agriculture, food, petrochemical, biomedicines, and other industries given its high efficiency, low cost, good reproducibility, and convenient application [11, 12]. Many researchers have used near infrared spectra technology to distinguish varieties and to measure component contents of products like waxberry and honey [13, 14]. Near infrared spectra technology has also been used to determine the origin and discriminate the gender of silkworm chrysalis and strains of *C. militaris* [15, 16]. The existing means for discrimination of infected silkworm chrysalis relies on experienced workers touching and pressing onto the surface of the silkworm chrysalis during cultivation of *C. militaris*. This process usually results in extensive contamination of silkworm chrysalises used for the culture, and is time consuming, laborious, and easily affected by workers' subjective bias. There is therefore an urgent demand for rapid and more effective discrimination of silkworm chrysalises. Given that the near infrared technology has the advantages of convenience, rapidity, and qualitative identification in areas pertaining to agriculture and food, it was used to discriminate the uninfected and infected silkworm chrysalises.

The objective of this study was to confirm whether near infrared spectroscopy can be used to identify the uninfected and infected silkworm chrysalises, and which part of the silkworm chrysalis is the ideal recognition part for fast and accurate discrimination of uninfected and infected silkworm chrysalises during the cultivation *of C. militaris*.

Experimental. *Antheraea pernyi* chrysalises, which were used as silkworm chrysalises, were provided by Beijing Shoucheng Agricultural Development Co., Ltd. Excluded in experiments were damaged, dead, shrunk, and poor-wing-cover silkworm chrysalises before inoculation. Each silkworm chrysalis was inocu-

lated with *C. sinensis* at the point of intersection between the rear wing and third segment (intersection of head and chest) on September 15, 2016. The process of inoculation will inevitably be contaminated by other microorganisms. Identification of silkworm chrysalises was carried out five days after the inoculation. On September 20, 2016, a total of 105 silkworm chrysalises—including 65 infected and 40 uninfected—were selected and identified by professionals for collection of near infrared spectra.

Near infrared spectra measurement. Near infrared absorbance spectra of silkworm chrysalises were acquired using a Luminar5030 spectrometer (Brimrose Co., Sparks, Nevada, USA) in the "Measurement modes" of absorbance. The equipment was composed of an optics parts, controller, power adapter, and a laptop. The spectrometer range was from 1100 nm to approximately 2500 nm, with a resolution of 2 nm. Silkworm chrysalises were put horizontally on the diffuse reflection probe of the spectrometer. For each silkworm chrysalis, spectra of the four positions, the head, chest, abdomen, and posterior belly were measured. Each site was scanned 10 times, and the average value of 10 measurements was taken as the spectra of each site. All acquired spectra of silkworm chrysalises were divided into modelling and prediction sets with a proportion of 1.6:1 using the kenned-stone method (KS). Among the 105 silkworm chrysalises, 45 infected chrysalises and 20 uninfected chrysalises were selected as a calibration set to build the discrimination models, while the rest, including 20 infected chrysalises and 20 uninfected chrysalises, were selected as a prediction set to validate the built models. In addition, the prediction set was also used to confirm which of the positions among the head, chest, abdomen, and posterior belly was the best discrimination part for the identification of uninfected and infected silkworm chrysalises. The temperature and relative humidity during the experiment were 21±1°C and 52.1±1%, respectively.

Pre-processing of spectral data. Spectral data of silkworm chrysalises were directly acquired through non-invasive detection, which possibly resulted in complicated background information. Therefore, original spectra probably contained high-frequency random noises, baseline drift, light scattering, and other noise information. The first-order derivative is normally used to eliminate constant baseline shifts, and the second-order derivative is used to eliminate the baseline slope [17]. By calculating the slope and the intercept between the spectrum of each detected object and the ideal spectrum, multiplicative scatter correction eliminates spectral scattering changes caused by factors such as particle size, refractive index, and particle size distribution of the object to be detected [18]. Both derivative processing and multivariate scatter correction are common spectral pre-processing methods. To reduce or eliminate noises in spectral acquisition, original spectra were pre-processed using first-order derivative (FD), second-order derivative (SD), and multiplicative scatter correction (MSC).

Model establishment and evaluation indexes. ChemDataSolution software (Dalian ChemDataSolution Information Technology Co. Ltd.) was used for near infrared spectral modelling. Principal component analysis combined with Mahalanobis distance (PCA-MD), partial least square discriminant analysis (PLS-DA), *k*-nearest neighbor algorithm (KNN), and support vector machine (SVM) are commonly used methods for qualitative identification in near infrared spectroscopy [19–21]. Thus, these methods were used to establish the recognition model for infected and uninfected silkworm chrysalises. Values of '0' and '1' were set as reference values for infected and uninfected silkworm chrysalises, respectively, during modelling. Qualitative models of PCA-MD, SVM, KNN, and PLS-DA were established via the scheme of leave-one-out cross validation. Qualitative models were evaluated using the recognition rates of modelling set and verification set and the accuracy of uninfected and infected silkworm chrysalises. Moreover, the recognition accuracy was selected as a key indicator to evaluate the performance of qualitative models.

Results and discussion. The original spectra of all silkworm chrysalises (including the uninfected and infected) are shown in Fig. 1. Each spectrum was the average of the spectra of four sites – the head, chest, abdomen, and posterior belly. As can be seen from Fig. 1, the spectral curves had a very similar shape, but there was a large variability in absorbance. All spectra had the same trend, and there was no abnormal spectrum that needed deleting. Average spectra of the two different silkworm chrysalises are shown in Fig. 2a. It is worth noting that the average spectra of uninfected and infected silkworm chrysalises showed three absorbance peaks, at 1400, 1770, and 1950 nm of the original spectrum. In spectral analysis, overlapping absorbance peaks were frequently observed in the original spectrum. First-order derivative (FD) processing method was usually used to separate the overlapping absorbance peaks. Figure 2b displays the FD spectra of uninfected and infected silkworm chrysalises, and there were six absorbance peaks at the region of 1320, 1400, 1660, 1710, 1750, and 1880 nm in the FD spectra. Those peaks, which existed in the original and FD spectra, were related with the main chemical components of silkworm chrysalis such as proteins, fats, fatty acids, and water [22]. The absorbance peak near 1320 nm was attributed to the second overtone region

of O–H. The absorbance peak near 1400 nm was related to the first overtones of C–H and O–H vibrations of methyl, methylene, and methine. The absorbance peaks near 1660 and 1710 nm were the first overtones of C–H of methyl and arene. The absorbance peak near 1750 nm was the first overtones of C–H and S–H. The absorbance peak near 1880 nm was the first overtones of water and esters [23]. The spectra of uninfected and infected silkworm chrysalises were different (Fig. 2a). The absorbance peak strength of the infected silkworm chrysalises was higher than that of the uninfected within the region from 1200 to 1350 nm, while the absorbance peak strength of the infected silkworm chrysalises was lower than that of the uninfected within the region from 1900 to 2050 nm. This was caused by the difference of internal chemical composition in uninfected and infected silkworm chrysalises as it was found that the infected chrysalises were festered, while the uninfected chrysalises were covered with *Cordyceps* mycelium during the cultivation of *C. militaris*. These absorbance peaks and differences were the spectroscopic basis for the discrimination of silkworm chrysalises using near infrared spectra.

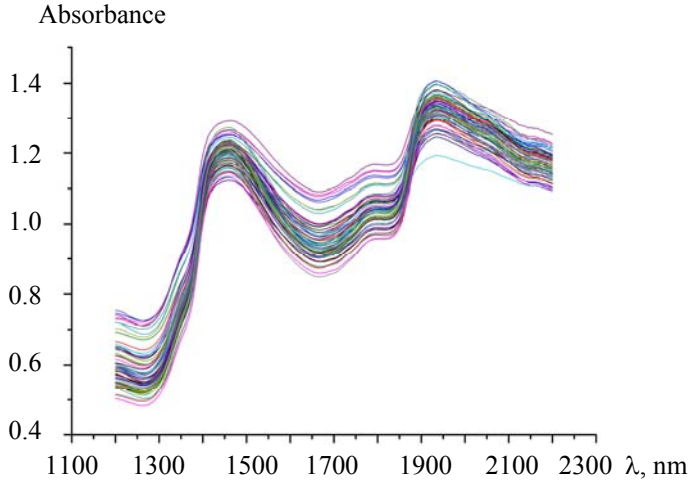

Fig. 1. The original spectra of all silkworm chrysalises including the uninfected and infected silkworm chrysalises.

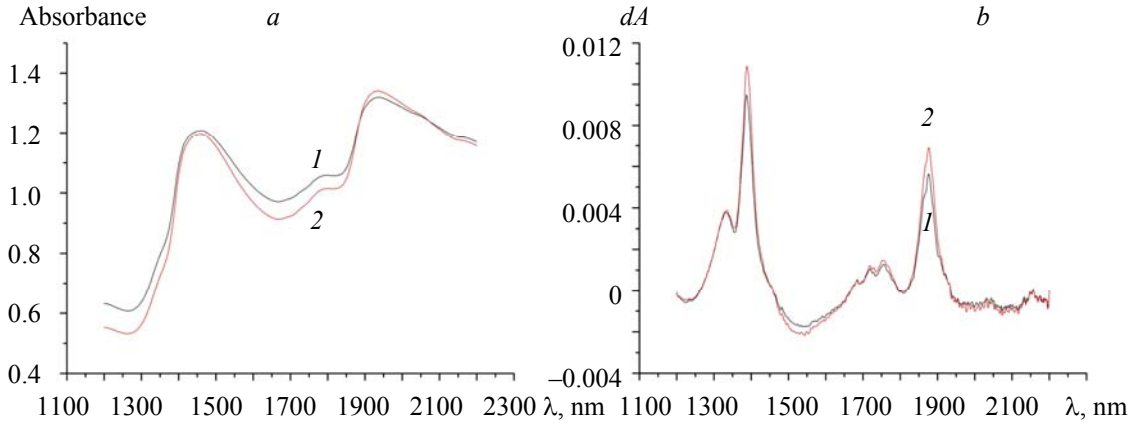

Fig. 2. Comparison of the original spectra and the first derivative spectra of infected and uninfected silkworm chrysalis. a) Average near infrared spectra of infected and uninfected silkworm chrysalises; b) first-order derivative of the average near infrared spectra of infected and uninfected silkworm chrysalises; represent the infected (1) and uninfected (2) silkworm chrysalis.

Building identification models. Sixteen qualitative models of PCA-MD, SVM, KNN, and PLS-DA were established using the pre-processed spectra of FD, SD, and MSC. The performance of all the models is shown in Table 1. As shown in Table 1, KNN model of the original spectra had the highest recognition rate

compared with the other modelling methods using the original spectrum, with the accuracy of 84.75%. PLS-DA models with FD, SD, and MSC spectra achieved the highest recognition rates compared with the other modelling methods.

The recognition performance with the original spectrum was poor compared with FD, SD, and MSC generally (Table 1). It was because substantial interference noise caused poor recognition effect of the qualitative recognition model of the original spectra. Spectral pre-processing could effectively eliminate spectral noises and thereby significantly increased spectral prediction [24]. The PLS-DA models had the best recognition performance compared with the other models because the PLS algorithm could extract the relevant information of the dependent *Y*-variables and the independent *X*-variables to the maximum extent. After comparing the 16 discrimination models, SD and MSC pre-processing was found to be suitable pre-processing methods, and the PLS-DA was selected as the optimal modelling method for the discrimination of uninfected and infected silkworm chrysalises. Thus, PLS-DA models with SD and MSC spectra were determined for further analysis.

TABLE 1. Classification Results of Silkworm Chrysalises in Calibration Set Based on Spectral Data

Pre-processing method	Modelling method	Recognition rate of uninfected, %	Recognition rate of infected, %	Accuracy, %
OS	PCA-MD	24.00	95.00	59.50
	SVM	56.00	80.00	68.00
	KNN	72.00	97.50	**84.75**
	PLS-DA	88.00	77.50	82.75
FD	PCA-MD	52.00	92.50	72.25
	SVM	0.00	100.00	50.00
	KNN	80.00	77.50	78.75
	PLS-DA	96.00	100.00	**98.00**
SD	PCA-MD	84.00	100.00	92.00
	SVM	0.00	100.00	50.00
	KNN	100.00	72.50	86.25
	PLS-DA	100.00	100.00	**100.00**
MSC	PCA-MD	24.00	100.00	62.00
	SVM	76.00	92.50	84.25
	KNN	60.00	85.00	72.50
	PLS-DA	100.00	100.00	**100.00**

N o t e. OS, FD, SD, and MSC represent the original spectrum, first-order derivative, second-order derivative, and multiplicative scatter correction, respectively.

Model validation and the determination of the best discrimination parts. The prediction set, including 20 uninfected and 20 infected silkworm chrysalises, was used to verify the model performances and determine which among the four positions (the head, chest, abdomen, and posterior belly) was the best discrimination part. Spectra of the head, chest, abdomen, and posterior belly of each silkworm chrysalis were used. As discussed above, PLS-DA models with SD and MSC spectra had the best discrimination performances, which was why SD and MSC pre-processing methods were used to pre-process the spectra of head, chest, abdomen, and posterior belly. PLS-DA models of uninfected and infected silkworm chrysalises were established and evaluated. Table 2 lists the results of PLS-DA models using the pre-processed spectra at four positions (the head, chest, abdomen, and posterior belly) of silkworm chrysalises. The PLS-DA model of head spectral data with MSC pre-processed had the highest recognition rate, with recognition rates for uninfected and infected silkworm chrysalises at 100 and 95%, respectively, and accuracy of 97.5%. The PLS-DA model of chest spectral data with MSC pre-processed had moderate recognition effect. The PLS-DA models of abdomen and posterior belly spectral data with SD pre-processed were poorly recognized. The different recognition rates of the four positions were caused by inoculation of *C. militaris.* During the cultivation of *C. militaris*, each silkworm chrysalis was inoculated with *C. sinensis* at the point of intersection between the rear wing and third segment (intersection of head and chest), while microbe contamination was unavoidable during inoculation. After inoculation, *C. sinensis* and microbes started growing from the inoculation point to

other parts of the silkworm chrysalis. In particular, they gradually spread from the head–chest intersection to other body parts of the worm. Therefore, recognition rates were higher at the head and chest of uninfected and infected silkworm chrysalises.

TABLE 2. Model Results of Silkworm Chrysalis in Prediction Set

Measurement position	Pre-processing	Recognition rate of uninfected, %	Recognition rate of infected, %	Accuracy, %
Head	SD	85	100	92.5
	MSC	100	95	**97.5**
Chest	SD	85	95	90
	MSC	95	85	90
Abdomen	SD	95	55	75
	MSC	80	100	**90**
Posterior belly	SD	95	55	75
	MSC	90	85	**87.5**

N o t e. SD and MSC represent the original spectrum, first-order derivative, second-order derivative, and multiplicative scatter correction, respectively.

The PLS-DA model with SD spectra at the head achieved recognition rates of uninfected silkworm chrysalises, infected silkworm chrysalises, and accuracy of 85, 100, and 92.5%, respectively, whereas corresponding values from the PLS-DA model with MSC spectra were 100, 95, and 97.5%, respectively. The recognition accuracy of PLS-DA model with SD spectra at the head was lower than that of the PLS-DA model with MSC spectra. Moreover, in terms of the recognition accuracy at four positions of the silkworm chrysalis, recognition performances at the head were better than at the other three positions (the chest, abdomen, and posterior belly). Thus, the head of silkworm chrysalis was the best discrimination part for both uninfected and infected silkworm chrysalises. The results indicate that the qualitative model based on the SD spectra was inferior to that based on the MSC spectra. Therefore, the PLS-DA model with MSC spectra was optimum for the recognition of uninfected and infected silkworm chrysalises during the cultivation of *C. militaris*, and the head of the chrysalis was found to be the best discrimination part. The scatter plot of the best model (PLS-DA model with MSC spectra at the head) for the discrimination of uninfected and infected silkworm chrysalises was plotted using the top two PCs (PC1 and PC2) of the prediction set of samples (Fig. 3).

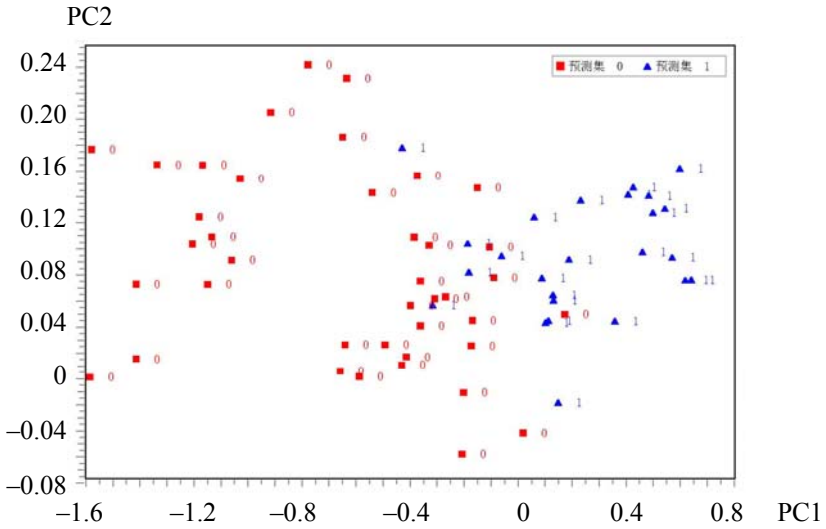

Fig. 3. Scatter plot of uninfected and infected silkworm chrysalises using PLS-DA model with MSC spectra at head; represent the infected (■) and uninfected (▲) silkworm chrysalises.

Discrimination of uninfected and infected silkworm chrysalises was successfully performed using near infrared spectra. Based on the results in this study, it appears that using near infrared spectroscopy in the production process of *C. militaris* cultivation could effectively reduce the labor cost and avoid property loss caused by the cross-contamination of infected silkworm chrysalis, owing to the rapid and accurate discrimination of infected silkworm chrysalises. It is also important for the quality monitoring of *C. militaris*. However, the cultivation process of *C. militaris* was complex since the internal chemical compositions of the infected silkworm chrysalises were different when compared with the uninfected silkworm chrysalises. Instead of involving other physical and chemical methods for determining the internal composition of infected and uninfected silkworm chrysalis, it is possible to select spectral variables while remaining within the framework of the chemometric approach to spectral data. Finding the differences in chemical composition between uninfected and infected silkworm chrysalises and screening out the sensitive bands associated with these chemical constituents could reduce the complexity of discrimination models. Moreover, this could also be helpful for the discrimination equipment development of infected silkworm chrysalis. Thus, further study should use near infrared spectra combined with other physical and chemical methods to find the main inner compositions determining the difference among the infected and uninfected silkworm chrysalises and to find the sensitive bands to reduce the model complexity.

Conclusions. In this study, application of near infrared spectra in recognition of uninfected and infected silkworm chrysalises was explored using different spectral pre-processing and modelling methods during the cultivation of *C. militaris*. The PLS-DA model with MSC spectra at the head of the silkworm chrysalis had the best discrimination performance, with recognition accuracy of 97.5% in model validation. It can be concluded that near infrared spectra can be used for the discrimination of uninfected and infected silkworm chrysalises, and the head of silkworm chrysalis was the best discrimination part. However, the use of the complete near infrared spectra in the modelling process caused a large amount of redundant information to be included. In order to meet the needs of the on-line and fast detection of uninfected and infected silkworm chrysalises, further research is needed to reduce the modelling variables by selecting sensitive wave bands that are related to the chemical differences between uninfected and infected silkworm chrysalises.

Acknowledgements. This work was supported financially by the Key-Area Research and Development Program of Guangdong Province (2019B020214005), the National Natural Science Foundation of China (31601216) and the Special Construction of Innovation Ability of Beijing Academy of Agriculture and Forestry Science (KJCX20170418). We also acknowledge the Key R&D and Promotion Project of the Henan Province (212102110207).

REFERENCES

1. G. H. Sung, N. L. Hywel-Jones, J. M. Sung, J. J. Luangsaard, B. Shrestha, J. W. Spatafora, *Stud. Mycol.*, **57**, 50–59 (2007).
2. S. X. Bi, Y. S. Jing, Q. Q. Zhou, *Food Funct.*, **9**, No. 1, 279–293 (2018).
3. K. Nakamura, K. Shinozuka, N. Yoshikawaa, *J. Pharmacol. Sci.*, **127**, No. 1, 53–56 (2015).
4. Z. Y. Zhu, F. Liu, H. Gao, H. Sun, M. Meng, Y. M. Zhang, *Int. J. Biol. Macromol. A*, **93**, 1090–1099 (2016).
5. X. W. Tian, Q. P. Song, M. He, Y. L. Lu, Y. C. Liu, L. S. Feng, *Biosci. Biotech. Res. Commun*., **9**, No. 4, 596–602 (2016).
6. H. T. Fan, H. S. Lin, *Chin. J. Chin. Mater. Med.*, **38**, 2549–2552 (2013).
7. H. O. Kim, J. W. Yun, *J. Appl. Microbiol.*, **99**, 728–738 (2005).
8. Z. L. Zheng, C. H. Huang, C. Y. Mei, R. C. Han, *J. Environ. Entomol.*, **33**, 225–233 (2011).
9. R. R. M. Paterson, *Phytochemistry*, **69**, 1469–1495 (2008).
10. Y. F. Han, *Microbiol. China*, **32**, 1423–1428 (2009).
11. X. L. Chu, W. Z. Lu, *Spectrosc. Spectr. Anal.*, **34**, 2595–2605 (2014).
12. H. Z. Chen, L. L. Xu, G. Q. Tang, Q. Q. Song, Q. X. Feng, *Food Anal. Methods*, **9**, 1–10 (2015).
13. Y. He, X. L. Li, *J. Infrared Millim. Waves*, **25**, 192–194 (2006).
14. H. E. Tahir, X. B. Zou, T. T. Shen, J. Y. Shi, A. A. Mariod, *Food Anal. Methods*, **9**, 2631–2641 (2016).
15. S. M. Pan, M. Tao, A. Q. Sun, T. M. Jin, *Acta Entomol. Sin.*, **39**, 360–365 (1996).
16. F. Dai, L.Wu, G. Ye, Y. Zhong, T. Hong, X. Huang, *Trans. Chin. Soc. Agric. Mach.,* **46**, No. 12, 280–284 (2015).
17. J. Engel, J. Gerretzen, E. Szymańska, J. Jansen, G. Downey, L. Blanchet, L. Buydens, *TrAC Trends*

Anal. Chem., **50**, 96–106 (2013).
18. R. Vašát, R. Kodešová, A. Klement, L. Borůvka, *Geoderma*, **298**, 46–53 (2017).
19. Y. Zhao, J. Zhang, H. Jin, J. Zhang, T. Shen, Y. Wang, *J. AOAC Int.*, **98**, 22–26 (2015).
20. B. T. Borille, M. C. Marcelo, R. S. Ortiz, K. C. Mariotti, M. F. Ferrão, R. P. Limberger, *Spectrochim. Acta A*, **173**, 318–323 (2016).
21. E. Teye, X. Huang, H. Dai, Q. Chen, *Spectrochim. Acta A*, **114**, 183–189 (2013).
22. L. L. Tao, W. Huang, X. J. Yang, Z. Y. Cao, J. M. Deng, S. S. Wang, F. Y. Mei, M. W. Zhang, X. Zhang, *Spectrosc. Spectr. Anal.*, **36**, 2766–2773 (2016).
23. T. Koumbi-Mounanga, K. Groves, B. Leblon, G. Zhou, P. A. Cooper, *Eur. J. Wood Prod*., **73**, 43–50 (2015).
24. F. Mabood, F. Jabeen, M. Ahmed, J. Hussain, S. A. A. Al Mashaykhi, Z. M. A. Al Rubaiey, S. Farooq, R. Boqué, L. Ali, Z. Hussain, A. Al-Harrasi, A. L. Khan, Z. Naureen, M. Idrees, S. Manzoor, *Food Chem.*, **221**, 746–750 (2017).